

Cite this: *J. Mater. Chem. B*, 2020,  
8, 4764

## Advances and challenges in metallic nanomaterial synthesis and antibacterial applications

Zengchao Guo,<sup>†</sup> Yun Chen,<sup>†</sup> Yihan Wang, Hui Jiang  and Xuemei Wang \*

Multi-drug resistant bacterial infection has become one of the most serious threats to global public health. The preparation and application of new antibacterial materials are of great significance for solving the infection problem of bacteria, especially multi-drug resistant bacteria. The exceptional antibacterial effects of metal nanoparticles based on their unique physical and chemical properties make such systems ideal for application as antibacterial drug carriers or self-modified therapeutic agents both *in vitro* and *in vivo*. Metal nanoparticles also have admirable clinical application prospects due to their broad antibacterial spectrum, various antibacterial mechanisms and excellent biocompatibility. Nevertheless, the *in vivo* structural stability, long-term safety and cytotoxicity of the surface modification of metal nanoparticles have yet to be further explored and improved in subsequent studies. Herein, we summarized the research progress concerning the mechanism of metal nanomaterials in terms of antibacterial activity together with the preparation of metal nanostructures. Based on these observations, we also give a brief discussion on the current problems and future developments of metal nanoparticles for antibacterial applications.

Received 12th January 2020,  
Accepted 25th February 2020

DOI: 10.1039/d0tb00099j

rsc.li/materials-b

### 1. Introduction

Humans have been fighting bacteria since ancient times. Pathogenic bacteria widely exist in the environment, with characteristics of variety, spreading quickly and easily causing adverse reactions. Infection caused by the invasion of bacteria into the human body is a severe threat of human diseases such as sepsis, pneumonia and gastritis. Since the invention of penicillin, antibiotics have made tremendous contributions to the fight against various pathogens. Nevertheless, with the abuse of antibiotics, bacteria have to make mutations to antibiotics and develop resistance, leading to the emergence of a large number of drug-resistant strains, which significantly reduces the therapeutic efficacy of antibiotics. Eventually, it leads to a severe multidrug-resistant (MDR) infection that poses a considerable threat to global public health security. Compared with the development speed of drug resistance, the development of new antibacterial drugs is not enough. According to Huh *et al.*, in the 21st century, only 1–2 new antibiotics were approved by the FDA for clinical use each year.<sup>1</sup> To make matters worse, after a period of application of new antibiotics, the corresponding resistant strains will also appear rapidly, causing the drug to be ineffective again. Clearly, it is fundamentally essential to explore novel antimicrobial strategies to fight bacterial infection.

Based on exceptional antibacterial performance and high specific surface area, nanomaterials have been widely studied by researchers all over the world as the most promising antimicrobial substances, and bacteria can hardly develop resistance owing to the complex antibacterial mechanism of nanomaterials (Fig. 1).<sup>2–5</sup> As an important branch of nanomaterials, metal nanomaterials with interesting magnetic, electrical, photothermal and other excellent physicochemical activities,<sup>6,7</sup> as a kind of popular materials, have been used as potential antimicrobial agents.<sup>8–11</sup> The latest research shows that in addition to antimicrobial drug loading, metal nanomaterials can also be used for bacterial infection detection and treatment.<sup>12–16</sup> The antibacterial properties of metal nanomaterials depend strongly on the size, shape and composition of their structures. To date, diverse methods have been developed to synthesize metal nanomaterials in a variety of shapes such as rods, clusters, cubes, spheres, cages, *etc.*<sup>17–23</sup> Among many metallic elements, gold and silver as “noble” metals have been the focus of various research areas in recent years. In this article, we will briefly review the synthesis strategies and possible antibacterial mechanism and challenges of some metal nanomaterials including Au and Ag.

### 2. Controlled synthesis of gold nanostructures

The performance of metal nanomaterials depends largely on the shape, size, composition, crystallinity and structure of

State Key Laboratory of Bioelectronics (Chien-Shiung Wu Lab), School of Biological Science and Medical Engineering, Southeast University, Nanjing 210096, China.

E-mail: xuemei@seu.edu.cn

<sup>†</sup> Common first author.

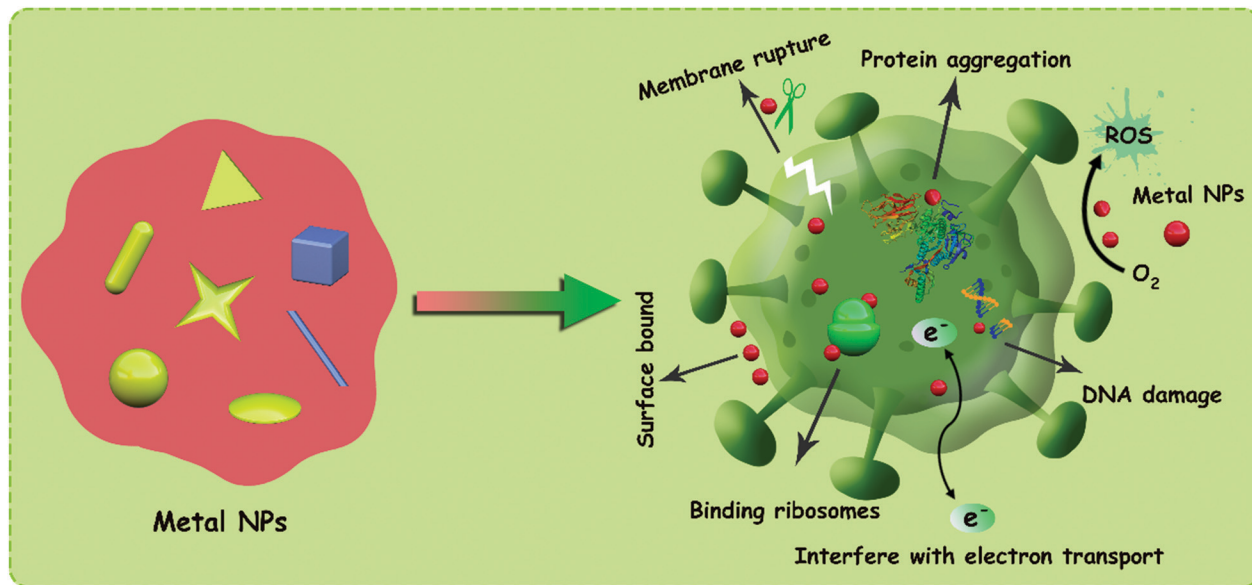


Fig. 1 Schematic diagram of the antibacterial mechanism of metal nanoparticles.

the particles.<sup>24,25</sup> Therefore, research on controllable synthesis of metal nanomaterials with multiple morphologies is the focus of nanomaterial preparation.

Since Faraday first discovered gold nanoparticles by employing a two-phase approach in 1857,<sup>26</sup> gold nanostructures (NPs) with various morphologies have been successfully synthesized through a variety of methods (Table 1).

At present, the simplest way to synthesize monodisperse, spherical gold nanoparticles is still to use sodium citrate to reduce chloroauric acid ( $\text{HAuCl}_4$ ) in an aqueous solution, which was reported by Turkevich *et al.* in the early 1950s.<sup>27,28</sup> They found that adding citrate to  $\text{HAuCl}_4$  could temporarily change the pH of the reaction medium, and then change the

nature of the  $\text{HAuCl}_4$  and therefore its reactivity. Xia *et al.* improved the traditional Turkevich method to prepare monodisperse, spherical gold NPs with sizes varying from 12 nm to 36 nm.<sup>29</sup> According to the famous LaMer model,<sup>30</sup> the brief separation of nucleation and growth steps is the crucial factor for the formation of monodisperse, spherical gold nanoparticles. In the method of seed-mediate growth, pre-formed small nanoparticles are not only used as the reduction catalyst, but also as the nucleation site (seed) of metal ions, which was widely used in the synthesis of monodisperse spherical gold NPs larger than 12 nm in size.<sup>31,32</sup> Liz-Marzán *et al.* reported that monodisperse spherical gold nanoparticles ranging in size from 12 nm to 180 nm were successfully synthesized by the seed

Table 1 Different types of gold nanomaterials

Au nanomaterials	Shape	Size range	Synthesis methods
Clusters		<3 nm	Etching, one-pot synthesis, electroreduction, photoreduction, bioreduction, microwave-assisted reduction
Spheres		5–230 nm	Seed-mediated growth
Rods		20 nm to several $\mu\text{m}$	Seed-mediated growth, electroreduction, photoreduction, bioreduction, microwave-assisted reduction, solvothermal reduction
Plates, prisms, and disks		40–1000 nm (edge length) and 5–50 nm (thickness)	Ultrasound-assisted reduction, microwave-assisted reduction, electroreduction, photoreduction
Shells		10–400 nm	Template-directed method
Boxes, cages, frames, and related hollow structures		20–200 nm (edge length)	Galvanic replacement reaction
Polyhedra		20–270 nm	Seed-mediated growth, polyol process
Structures with branched arms		45–300	Seed-mediated growth, one-pot synthesis

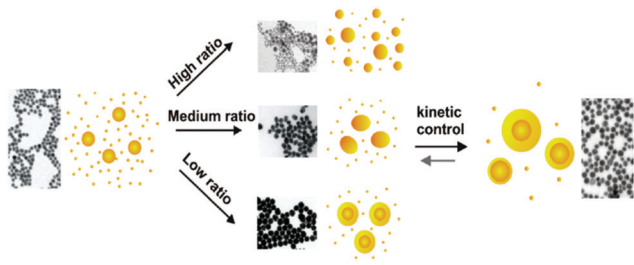


Fig. 2 Illustration of the different growth pathways for the kinetically controlled seeded growth of Au NPs.<sup>34</sup>

growth method, and hexadecyl trimethylammonium bromide (CTAB) was used as the capping agent to control the growth of nanoparticles.<sup>33</sup> Puentes *et al.* synthesized spherical gold nanoparticles with highly monodisperse and uniform size by reducing  $\text{HAuCl}_4$  with sodium citrate and controlling the growth process of seeds by kinetics (Fig. 2).<sup>34</sup> Liu *et al.* reported a simple, rapid and surfactant-free method of synthesizing spherical gold nanoparticles with sizes ranging from 12 nm to 230 nm using hydrogen peroxide as a reducing agent.<sup>35</sup>

In addition to spherical gold nanoparticles, anisotropic gold nanomaterials, such as gold nanorods (NRs), are of considerable interest because they exhibit better chemical and physical properties than spherical gold NPs. Among the methods, the seed-mediated growth method requires less equipment and the preparation process is simple, and it has received the most extensive attention and become the primary method of wet chemical synthesis of gold NRs. The seed-mediated growth method mainly includes two steps. The first step is to prepare small-size seeds, which are generally smaller than 10 nm. The second step is to add seeds into the growth solution as inducing agents. The preparation of the growth solution is generally obtained by reducing chlorauric acid (salt) with weak reductants (such as hydroxylamine and ascorbic acid).

The seed growth method was first developed by Murphy's group; the main drawback is the low yield.<sup>36</sup> To overcome the problem, they then refined the process so that the yield reached 90%.<sup>37</sup> Later, Huang *et al.* improved Murphy's method and obtained gold nanorods with a narrow size distribution and high yield after adding  $\text{HNO}_3$  into the growth solution.<sup>38,39</sup> Based on these studies, Nikoobakht *et al.* proposed the theory of  $\text{Ag}^+$  assisted growth and further improved this method.<sup>40</sup> Subsequently, researchers extensively studied the specific conditions in detail, and Jana *et al.* found that the seed size had an important effect on the symmetry of the Au NRs.<sup>41</sup> Park *et al.* believed that the by-products of gold nanorods synthesized by the seed growth method were mainly caused by insufficient understanding of the early growth of gold nanorods.<sup>42</sup> In addition to the typical capping agent CTAB, a large number of other additives have also been introduced into the process of preparing gold nanorods by the seed growth method, such as copper ions,<sup>43</sup> aromatic additives,<sup>44</sup> sodium oleate<sup>45</sup> and so on. Jiang *et al.* added  $\text{AgNO}_3$  into the solution to promote the reaction; they prepared gold nanorods with a narrow size distribution, and the volume of gold NRs accounted for 79% of the whole product.<sup>46</sup>

Meanwhile, as a bridge between individual atoms and large plasmonic nanoparticles, ultrasmall noble metal nanoparticles with core size less than 3 nm that contain few atoms are another exciting research area that deserves special attention.<sup>47,48</sup> In order to gain high-quality Au NCs, the reducing condition should be strict, and the ligand should have reliable interaction with metal NCs. Small thiol molecules were first used to prepare Au NCs by reduction of a Au precursor with  $\text{NaBH}_4$ .<sup>49,50</sup> The fluorescence emission of these gold nanoclusters can be effectively regulated from the blue region to the near-infrared region (NIR). A poly(amidoamine) dendrimer, as another attractive ligand, has also been employed to synthesize Au NCs with  $\text{QY} > 10\%$ .<sup>51</sup> Furthermore, Santiago *et al.* reported the synthesis of Au NCs with only 2–3 atoms by a simple electrochemical method using polyvinylpyrrolidone (PVP); the Au NCs also had magnetic properties.<sup>52</sup> Due to the expensive synthesis process or the use of toxic reagents, utilizing biological ligands can effectively decrease the possible toxicity of Au NCs and increase their suitable applications in biomedicine. Using bovine serum albumin (BSA) as a bio-ligand, Xie *et al.* synthesized Au NCs with red emission by using a simple, one-pot, "green" synthetic route at physiological temperature as shown in Fig. 3.<sup>53</sup> Lysozyme is also a better reducing agent; Wei *et al.* employed lysozyme as a friendly reagent for the synthesis of highly fluorescent Au NCs.<sup>54</sup> In addition, both DNA<sup>55,56</sup> and proteins such as pepsin,<sup>57</sup> lactoferrin,<sup>58</sup> trypsin<sup>59</sup> and papain<sup>60</sup> can also be used as ligands to synthesize Au NCs. In recent years, *in situ* biosynthesis of gold nanoclusters has attracted a wealth of attention, due to its biocompatible and economic nature and low-toxicity. Wang's group conducted pioneering research and reported that fluorescent gold nanoclusters are spontaneously biosynthesized by cancerous cell when incubated with micromolar  $\text{HAuCl}_4$  solutions.<sup>61–63</sup> Furthermore, Goswami *et al.* synthesized gold nanoclusters on a bacterial template for enumeration and detection of bacterial contaminants and kanamycin-resistant strains.<sup>64</sup>

Based on these studies, Chen *et al.* improved the seed growth method; by controlling the proportion of seeds and growth solution and adding other ions, gold nanoparticles with different morphology including spherical, rod-shaped, fusiform, star-shaped and triangular shaped could be obtained. Temperature has a significant effect on the product. As can be seen from Fig. 4, when the temperature changes between 40 °C and 90 °C, the products transition from rod shape to triangle shape and finally

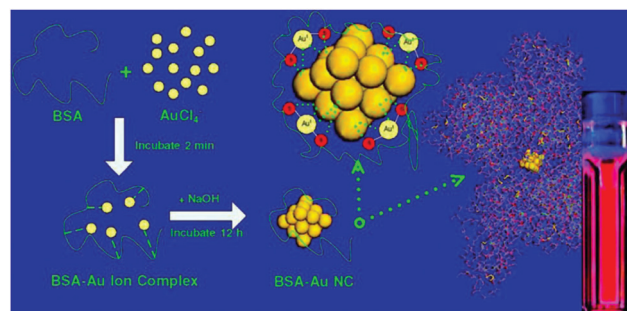


Fig. 3 Green synthesis of BSA–Au NCs.<sup>53</sup>

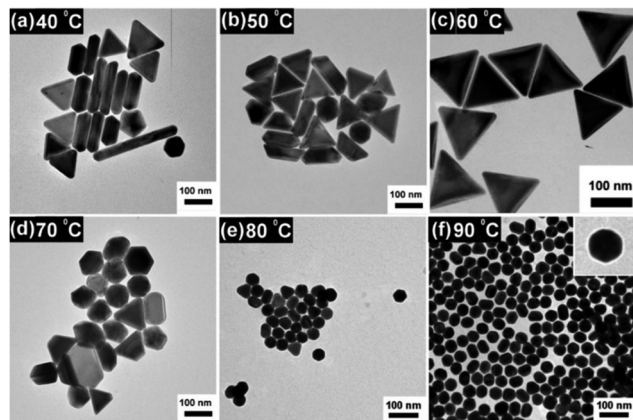


Fig. 4 (a–f) TEM images of Au nanoparticles at various temperature conditions as labeled in each image.<sup>65</sup>

become spherical products.<sup>65</sup> Shao *et al.* adopted the method of aspartic acid reduction for  $\text{HAuCl}_4$ , and obtained a large number of gold nanoparticles with triangular, hexagonal and irregular flake structure particles.<sup>66</sup>

Among special morphologies, many studies have been done on gold nanoparticles with multiple branches. Compared with the traditional spherical and rod-shapes, they have a larger specific surface area, and their high activity and sharp edge structure can be modified to a superhydrophobic surface and oil-phobic surface, as well as sizeable magnetic field enhancement, *etc.*, which brings enormous potential applications, such as electrocatalysis, SERS, surface plasma and others.<sup>67–69</sup> The methods of preparing gold nanostructures with branched arms include gas phase polymerization,<sup>70</sup> ultrasound-assisted methods,<sup>71</sup> hydrothermal methods<sup>72</sup> and so on. Yamamoto *et al.* prepared star-shaped gold nanoparticles by reduction of polyvinyl-2-pyrrolidone.<sup>73</sup>

### 3. Typical strategies of synthesizing silver nanomaterials

The experimental conditions of synthesis determine the morphology, size and stability of silver nanoparticles.<sup>74</sup> In the last decades, the controllable synthesis of silver nanoparticles has been developed rapidly. The synthesized silver nano-morphologies include spherical, cubic, wires, rods, discs, pyramids, triangular, *etc.*<sup>75–78</sup>

So far, different synthesis methods of silver nanocubes have been reported, including wet chemistry, hydrothermal synthesis and polyol methods. Chao *et al.* prepared silver nanocubes by a seed-assisted wet chemistry method. With the help of similar lattice constants of Ag and Pt, they induced the synthesis of silver nanocubes by using single crystal Pt seeds, and effectively adjusted the size of the silver nanocubes by changing the content of the seeds.<sup>79</sup> However, this method is very complicated and has low yield, which limits its practical application. Chang *et al.* proposed a hydrothermal method to synthesize high-quality silver nanocubes. They took cetyltrimethylammonium bromide (CTAB) as an inducer, ammonia as a complexing agent, silver

nitrate as a silver source and glucose as a reducing agent, and heated water at 120 °C to form silver nanocubes with a size of  $9.3 \pm 4.1$  nm.<sup>80</sup>

Actually, the preparation of nanocubes by the polyol process reported by Xia's research group is the biggest breakthrough and has been widely used in the synthesis of silver nanocubes.<sup>81–83</sup> They prepared silver nanocubes with high quality and high yield by an oil bath polyol method, and the size of the silver nanocubes could be controlled. It has been found that silver nanocubes are single crystal structures, but the product of pyramid and nanowire structures is easily obtained in the traditional polyol process, which is due to the formation of seeds of twinned structure in the initial stage. In order to obtain high purity silver single crystal seeds, twinned seeds must be oxidized and etched into single crystal seeds at the beginning of the reaction. Jeon *et al.* reported an improved oil bath polyol process in which hydrochloric acid was added to form a strong nitric acid oxidizing agent and  $\text{O}_2/\text{Cl}^-$  etching agent to etch and dissolve the twinned seeds into pure single crystal seeds in the initial stage, and finally get silver nanocubes of uniform size and shape.<sup>84</sup>

The synthesis of silver nanowires is another exciting research field that deserves special attention. Many methods can be used to effectively synthesize Ag NWs, such as wet chemistry, template, hydrothermal and polyol methods. The template method is an essential technique for synthesizing silver nanowires, mainly including cationic alumina (AAO), nanotubes, biological DNA and so on. The template can prevent agglomeration between the Ag NWs during the growth process, and can effectively control the orientation, size and morphology of the Ag NWs. Braun *et al.* first reported the synthesis of conductive Ag NWs by a DNA template method, which used ion exchange to load the DNA with silver ions, and the silver was collected on the DNA skeleton by reduction. Then, Ag NWs with a diameter of 100 nm and length of 12  $\mu\text{m}$  were prepared in citric acid buffer solution.<sup>85</sup> Park *et al.* designed a three-dimensional helical beam DNA structure and used it as a template to synthesize Ag NWs with a diameter of 20 nm.<sup>86</sup> Yang *et al.* synthesized nanowires with cationic alumina (AAO) as a template and obtained nanowires with a diameter of 35 nm.<sup>87</sup> Kim's group used calixarene-4-hydroquinone (CHQ) nanotubes as templates and combined with ultraviolet radiation technology to prepare nanowires with a diameter of 0.4 nm and length of up to microns. The method is carried out under normal temperature and pressure, which solves the previous problem of high temperature and high pressure in the preparation of nanowires and improves the stability of the products.<sup>88,89</sup> Although the template method is relatively controllable, there are some problems such as difficulty in template removal and aggregation of nanowires after template removal, which lead to the limitation of application of the prepared nanowires. The wet chemistry method generally synthesizes silver nanowires in a liquid phase system (such as water) under the action of a reducing agent and structure directing agent. With ascorbic acid as the reducing agent, PMMA as the coating agent and water as the solvent, Zhang *et al.* synthesized nanowires with a diameter of 30–40 nm.<sup>90</sup> Zhang *et al.* used a wet chemistry



method to reduce  $\text{AgNO}_3$  at  $100^\circ\text{C}$  with  $\text{Cu}_2\text{O}$  as a reducing agent and structure-guiding agent and water as a synthetic solvent to prepare nanowires with a diameter of about 50–500 nm and a length up to several tens of microns.<sup>91</sup> The hydrothermal method is to add a polymer surfactant to induce the growth of silver nanowires along the one-dimensional direction in an aqueous phase system, so as to realize the directional growth of silver nanowires and thus synthesize silver nanowires with a high length–diameter ratio. At the same time, the relatively closed environment also makes the product purer. Wang *et al.* mixed  $\text{AgNO}_3$  and  $\text{NaCl}$  in aqueous solution and used glucose as a reducing agent to prepare silver nanowires with higher purity.<sup>92</sup> Caswell *et al.* prepared silver nanowires about 12 nm long in an alkaline solution of sodium hydroxide with sodium citrate as a reducing agent without introducing crystal seeds and a surfactant.<sup>93</sup>

Compared with the above preparation methods, the polyol method can control well the morphology and size of nanomaterials. It is easy to operate, environmentally friendly, and produces a high length–diameter ratio and purity of silver nanowires. In short, the polyol method is to use polyols (EG, DEG, *etc.*) as a solvent or reducing agent, add a surfactant (such as PVP) as a dispersion stabilizer and inducer, and reduce the silver precursor to obtain silver nanowires at a certain temperature. Sun *et al.* introduced Ag or Pt crystal seeds into ethylene glycol solvent and synthesized silver nanowires with a diameter of 30–40 nm and a length of 50 nm with PVP as the structure guide.<sup>94</sup> In this method, silver nanowires of different sizes can be obtained by controlling the ratio of PVP/ $\text{AgNO}_3$ . Xia's team prepared 100 nm silver nanowires by introducing  $\text{NaCl}$  and  $\text{KCl}$ . They found that under the condition of high concentration of  $\text{Cl}^-$ ,  $\text{Cl}^-$  acted with oxygen atoms in the system to inhibit the formation of nanowires.<sup>95</sup> The researchers then studied the effect of metal ions ( $\text{Cu}^{2+}$ ,  $\text{Fe}^{3+}$ ) on the reaction products. Korte *et al.* studied the effects of  $\text{CuCl}_2$ ,  $\text{Cu}(\text{NO}_3)_2$  and  $\text{CuCl}$  on the products, and concluded that  $\text{Cu}^{2+}/\text{Cu}^+$  could prevent the etching of silver nanowires by  $\text{O}_2$  and promote the growth of silver nanowires, as shown in Fig. 5.<sup>96</sup> Ma *et al.* rapidly prepared silver nanowires with a diameter of 80–323 nm by adjusting the

$\text{FeCl}_3$  concentration at a high  $\text{AgNO}_3$  concentration.<sup>97</sup> In addition, Lee *et al.* made silver nanowires with a diameter of 120 nm and a length of 400–500 pm by a continuous multi-step polyol method, using glycol as the reducing agent and solvent,  $\text{AgNO}_3$  as the silver source and PVP as the surfactant.<sup>98</sup> Ran *et al.* prepared silver nanowires with a length–diameter ratio over 1000 by the polyol method. In this method, they introduced a mixture of surfactants pvp-k30 and -k90, which could adjust the size of the silver nanowires by changing the proportion of PVP of two different degrees of polymerization.<sup>99</sup>

Besides these studies, silver nanoclusters with photoluminescence were discovered as early as the 1980s, but early researchers synthesized silver nanoclusters only in the solid and gas phases, such as zeolites,<sup>100–102</sup> cryogenic inert gas<sup>103–105</sup> and inorganic glass.<sup>106,107</sup> In the 1990s, Henglein's group synthesized silver nanoclusters in the liquid phase for the first time, studied their physical and chemical properties in detail, and clearly pointed out that silver nanoclusters have non-metallic properties.<sup>108–114</sup> However, the synthetic water-soluble silver nanoclusters can only be stabilized for several hours, and fluorescence properties have not been reported. In 2002, Dickson and his team used a dendrimer as a template to synthesize stable water-soluble silver nanoclusters for the first time, which opened the research boom of silver nanoclusters.<sup>115</sup>

The branching structure of a polymer facilitates the formation of pores that protect the silver nanoclusters from agglomeration. Zheng *et al.* conducted pioneering research and synthesized stable silver nanoclusters for the first time with hydroxy-capped PAMAM as a ligand.<sup>115</sup> Lesniak *et al.* further demonstrated that the silver nanoclusters synthesized with PAMAM as a template have excellent biocompatibility and can be used as markers of cells.<sup>116</sup> Since it has been found that high density carboxyl groups contribute to the synthesis of silver nanoclusters, poly(methacrylic acid) (PMAA), a common and commercially available polymer, has also been used as a template for the synthesis of silver nanoclusters. Dong and his team first reported the synthesis of silver nanoclusters emitting red fluorescence through ultraviolet radiation (365 nm) using PMAA as a template and the silver nanoclusters were used to determine  $\text{Cu}^{2+}$ .<sup>117,118</sup> Subsequently, Liu *et al.* synthesized silver nanoclusters using PMAA as a template by a microwave irradiation method and used them to determine  $\text{Cr}^{3+}$ .<sup>119</sup> In addition, Yuan *et al.* synthesized blue-green fluorescent hPEI-AgNCs with hyperbranched polyethylenimine (hPEI) as the ligand and ascorbic acid as the reducing agent; the nanocluster has excellent pH stability and can be used for the detection of  $\text{Cu}^{2+}$  (Fig. 6).<sup>120</sup>

Small molecule compounds such as mercaptosuccinic acid, glutathione and other structures containing sulfhydryl groups have a strong complexation ability to silver ions, protect Ag NCs against agglomeration, and can also be used as ligands to synthesize silver nanoclusters. Wu *et al.* first synthesized silver nanoclusters using 2,3-dimercapto succinic acid (DMSA) as the template.<sup>121</sup> Subsequently, dihydrolipoic acid was also used as a template for the synthesis of silver nanoclusters that emitted red fluorescence and were used for the determination of  $\text{Hg}^{2+}$  (Fig. 7).<sup>122</sup> Pradeep *et al.* used mercaptosuccinic acid ( $\text{H}_2\text{MSA}$ ) as a template to obtain silver clusters with different numbers of

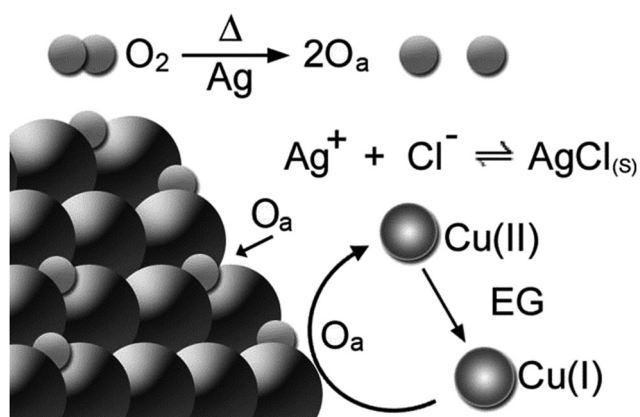


Fig. 5 Schematic illustration depicting the role of  $\text{Cu}^{2+}$  in the polyol synthesis of Ag nanowires.<sup>96</sup>

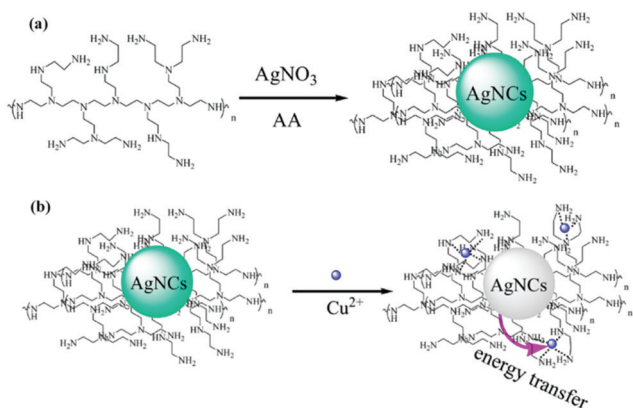


Fig. 6 (a) Synthetic strategy of hPEI-AgNCs and (b) hPEI-AgNC-based nanoprobe for the detection of  $\text{Cu}^{2+}$ .<sup>120</sup>

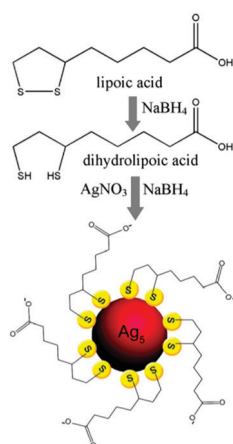


Fig. 7 The formation of an Ag nanocluster–DHLA nanoconjugate.<sup>122</sup>

atoms ( $\text{Ag}_7$ ,  $\text{Ag}_8$ <sup>123</sup> and  $\text{Ag}_9$ <sup>124</sup> nanoclusters) through different reaction pathways. Yuan *et al.* developed a reverse transfer method with sulfhydryl compounds as ligands, that is, after chemical reduction in the water phase, the system was transferred to ethanol for slow etching, and the synthesized silver nanoclusters had better dispersion, ultra-high stability and ultra-small size.<sup>125</sup> Zhu *et al.* synthesized GSH-Ag NCs with blue and red double emission fluorescence. When the concentration ratio of GSH and  $\text{Ag}^+$  changed during the synthesis process, the fluorescence intensity of the double emission peak changed accordingly.<sup>126</sup>

The high affinity of DNA to metal ions is mainly due to the strong interaction between metal ions and heterocyclic rings of bases.<sup>127</sup> There are many advantages of using DNA as a template to synthesize silver nanoclusters. For example, the synthesized silver nanoclusters have high fluorescence quantum yield, and the size and fluorescence emission wavelength of the silver nanoclusters can be controlled by adjusting the DNA base sequence. Petty *et al.* first synthesized fluorescent silver nanoclusters with single-stranded DNA of 12 bases (5'-AGGTCGCCGCC-3') as a template under  $\text{NaBH}_4$  reduction, and proved that there was a strong binding force between  $\text{Ag}^+$  and cytosine, as shown in Fig. 9a.<sup>128</sup>

Since  $\text{Ag}^+$  has different affinities with the four bases, the fluorescence properties of silver nanoclusters can be regulated by changing the sequence of DNA. Richards *et al.* used gene chip technology to optimize five single chain sequences, which can be used to synthesize silver nanoclusters with different fluorescence emission, with emission wavelength from the visible region to the near-infrared region.<sup>129</sup> Eun *et al.* used melamine to improve the fluorescence intensity and stability of DNA-silver nanoclusters. The results exhibited a *ca.* 3-fold larger fluorescence efficiency and long-term stability (70 d) in contrast to those of DNA-Ag NCs in the absence of melamine (Fig. 8).<sup>130</sup> Besides, double-stranded DNA can also be used for the synthesis of silver nanoclusters. Guo *et al.* designed a specific sequence of double-stranded DNA in which a cytosine-rich hairpin structure was inserted as a template for the synthesis of silver nanoclusters (Fig. 9b).<sup>131</sup> The silver nanoclusters were found to be highly sequence-dependent and specifically recognize gene mutations of sickle cell anemia. Subsequently, Ma *et al.* found that the mismatched base sites of double-stranded DNA could specifically grow silver clusters.<sup>132</sup> Gwinn and his team studied the dependence of the fluorescence of silver nanoclusters on the secondary structure of DNA, and for the first time synthesized four kinds of silver nanoclusters by regulating the number of cytosines using hairpin DNA as a template.<sup>133</sup>

In addition to the above-mentioned silver nanocubes, silver nanowires and silver nanoclusters, other silver nanostructures such as nanospheres, nanosheets and nanotubes have also been facily obtained through different methods. These different morphology silver nanomaterials exhibit different electrical, thermal and optical properties, which enriches the applications of silver nanomaterials.

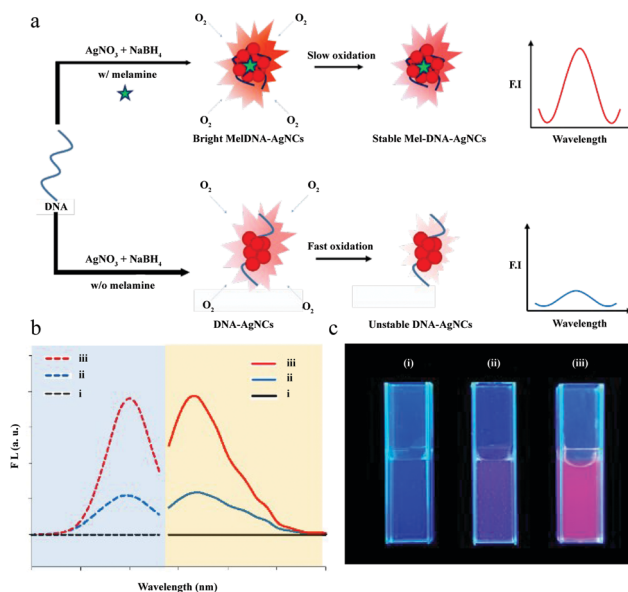


Fig. 8 (a) Illustration of melamine-promoted formation of Mel-DNA-Ag NCs with improved fluorescence properties. (b) Fluorescence excitation and emission spectra and (c) fluorescence images under UV light of solutions formed in the absence of the DNA template (i – black), in the presence of the DNA template (ii – blue), and in the presence of the DNA template together with melamine (iii – red).<sup>130</sup>

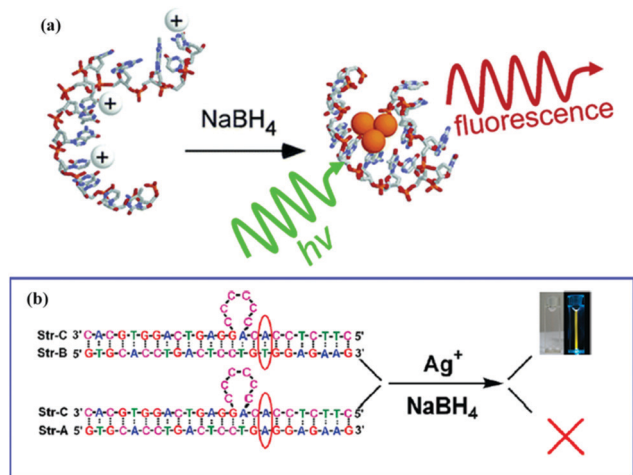


Fig. 9 (a) The formation of Ag nanoclusters using a DNA oligonucleotide as a scaffold<sup>128</sup> and (b) use of two different DNA duplexes with inserted cytosine loops working as synthetic scaffolds to generate fluorescent Ag nanoclusters.<sup>131</sup>

## 4. Antibacterial mechanism of Au/Ag NPs

Metal nanomaterials including Au NPs and Ag NPs have different antibacterial effects due to their surface modification, structure, shape, size, *etc.* The antibacterial mechanism of Au NPs is attributed to the following two aspects: (1) the effect on bacterial membranes with a change of the membrane potential and a decrease of the ATP level and (2) the function of entering into bacterial cells (Fig. 10).<sup>134</sup>

Au NPs with high specific surface area were modified to interact with proteins on the surface of bacterial membranes. Different proteins expressed on different bacterial surfaces had little effect on Au NP adhesion to the bacterial membrane surface. Studies have shown that Au NP aggregation on different bacterial surfaces was observed to differ only in morphology and amount, but the effect was similar.<sup>135</sup> Li *et al.* treated bacteria with Au NPs and then bleached and developed them with propiridine iodide (PI); significant destruction of the bacterial membranes was found. Thus, the modified Au NPs could accumulate on the bacterial membrane and affect its stability and integrity.<sup>136</sup>

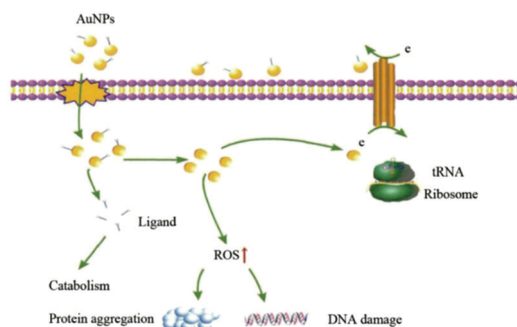


Fig. 10 Antibacterial mechanism of Au NPs.

Meanwhile, the intracellular antibacterial activities of Au NPs include the effects of its adjuvant antibacterial agents and its own antibacterial activities. Au NP-assisted antibacterial agents play a major role by carrying high concentrations of antibacterial drugs such as small molecule antibiotics, antimicrobial peptides and amphoteric cationic ligands into the cell through the uptake of bacteria.<sup>137–141</sup> The combination of Au NPs with antibacterial agents reduces the resistance of the bacterial membrane physical barrier to antibacterial drugs and improves the efficiency of the entry of antibacterial drugs into bacteria. For example, our previous study demonstrated an active antibacterial hybrid formed by covalently conjugating Au NCs and daptomycin. The as-synthesized hybrid structure could effectively disrupt bacterial membranes (Fig. 11), lead to more serious damage of bacteria at subcellular levels and limit the ability of bacteria to develop drug resistance.<sup>142</sup>

On the other hand, Au NPs enter the cell, and they can exert antibacterial effects in two ways: (1) they inhibit the binding of ribosome subunits to transport RNA (tRNA) and interfere with DNA transcription and replication<sup>134</sup> and (2) they produce a large amount of ROS aggregation. Au NPs interfere with the expression of metabolism-related genes, such as up-regulation of metabolic enzymes that promote oxidation and down-regulation of antioxidant genes, leading to the production of large amounts of peroxides and superoxides in the cells. Recent studies have shown that Au NPs exhibit antimicrobial activity by inducing intracellular oxidative stress injury. The survival rate of bacteria can be increased by using an antioxidant to antagonize ROS or reducing the temperature of the bacterial culture to inhibit its metabolic process.<sup>143</sup> Bing *et al.* indicated that the Au NPs could

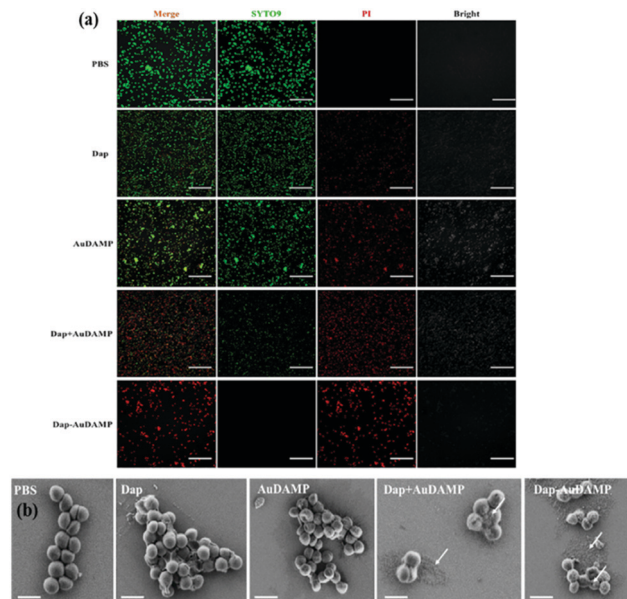


Fig. 11 (a) CLSM images of MRSA treated with PBS, Dap, AuDAMP, Dap + AuDAMP, and Dap-AuDAMP. The dead cells were visualized by PI staining (red), while SYTO 9 (green) was used to identify all cells. (b) SEM micrographs of bacteria treated with PBS, Dap, AuDAMP, Dap + AuDAMP, and Dap-AuDAMP.<sup>142</sup>



catalyze the decomposition of the naturally existing  $\text{H}_2\text{O}_2$  being produced by bacteria into  $\cdot\text{OH}$  and  $\text{O}_2^-$ . Owing to the excellent antibacterial capacity of ROS, the Au NPs exhibited striking antibacterial properties. Consequently, Au NPs can cause bacterial death by producing a large amount of intracellular ROS, which leads to intracellular protein aggregation and DNA destruction.<sup>144</sup>

In fact, the antibacterial mechanism of gold nanoparticles is a continuous process. Zheng *et al.* synthesized gold nanoclusters with mercaptoprimidine as ligands and uncovered that Au NCs could effectively damage the bacterial cell membranes and change their permeability. The change in cell membrane permeability then allowed Au NCs to easily internalize into bacterial cells, inducing the destruction of bacterial genomic DNA. More importantly, Au NCs could strongly induce intracellular ROS production after their entry. Furthermore, they further revealed the potential of Au NCs for *in vivo* applications both in a macrophage infection model and a mouse infection model and reported that the amount of bacteria was decreased significantly and all mice survived after 6 days of Au NC therapy.<sup>145</sup> Xie *et al.* reported that Au NCs significantly affect the bacterial cell membrane, including the membrane integrity, permeability, and inner potential, and observed a dramatic increase in the ROS levels and a decline in the ATP levels. They also demonstrated the potential application of Au NCs to combat bacterial infections *in vivo*. A low dose of Au NCs is efficacious for bacteria elimination and wound healing in a mouse skin infection model and the Au NCs do not cause an inflammatory response in mice, showing a good therapeutic effect in animal infection models.<sup>146</sup>

Compared with the antibacterial effect of Au NPs, silver nanoparticles have broad-spectrum antibacterial properties and do not produce drug resistance. They have a bactericidal effect on various microorganisms such as *Escherichia coli*, *Candida albicans* and *Staphylococcus aureus*. Studies have shown that they mainly exert antibacterial effects by releasing silver ions and producing ROS. The mechanism of action is shown in Fig. 12.<sup>147</sup>

Although different types of Ag nanoparticles have different toxicity mechanisms, the release of ions by nanoparticles is

usually an important step in the performance of nanotoxicity. In early studies, cysteine was added to cells that were exposed to Ag NPs. Since cysteine can bind to  $\text{Ag}^+$  and block the toxic effects of  $\text{Ag}^+$ , the antibacterial properties of the Ag NPs decreased significantly after adding cysteine, indicating that the toxicity of the Ag NPs comes from the release of  $\text{Ag}^+$ .<sup>148,149</sup> It is currently believed that silver ions can bind to electron donors in biomolecules containing sulfur, oxygen, or nitrogen and directly act on cellular enzymes and proteins, affecting cellular respiration and ion transmembrane movement, ultimately leading to cell death.<sup>150–152</sup>

Another important mechanism of silver toxicity is the generation of ROS by Ag NPs and their induced oxidative stress or oxidative damage. Abnormal accumulation of ROS induces oxidative stress. Reactive oxygen species can attack cell membranes, react with fats, proteins and nucleic acids, and hinder the cell transport system, leading to DNA damage and cell death.<sup>153</sup> Danilczuk *et al.* found free radicals generated by silver nanoparticles through the electron spin resonance spectrum.<sup>154</sup> Kim *et al.* observed the same results and found that the addition of the antioxidant *N*-acetylcysteine in the medium could counteract the bactericidal effect of Ag NPs, proving that the free radicals generated by Ag NPs were related to their antibacterial properties.<sup>155</sup>

It is evident that Ag NPs can accumulate on the cell membrane, attack the phospholipid bilayer of the cell membrane, and form bumps and holes in the cell membrane, causing material loss within the cell. Escárcega-González *et al.* demonstrated that membrane integrity is compromised either directly or as a consequence of the antimicrobial properties exhibited by Ag nanoparticles. They also found that the Ag NPs were capable of eradicating pathogenic resistant bacteria in an infection *in vivo* safely and efficiently.<sup>156</sup> As for the direct injury of the cell membrane by Ag NPs, Raffi *et al.* believed that it was due to the charge interaction between negatively charged bacteria and positively charged nanoparticles,<sup>157</sup> while Morones *et al.* believed that the silver nanoparticles bound to the thiol group of proteins on the cell membrane.<sup>158</sup> Sondi *et al.* found that Ag nanoparticles adsorbed on the cell membrane and accumulated, leading to the increase of cell permeability and intracellular substances flowing out of the cells, eventually leading to bacterial death.<sup>159</sup> Other researchers have also found that treatment of bacteria with silver nanoparticles results in the partial release of chromosome fragments due to cell membrane damage.<sup>160</sup> Furthermore, Ag NPs would also affect the membrane vesicles. Li *et al.* indicated that the membrane vesicles were dissolved and dispersed after *E. coli* exposure to Ag nanoparticles.<sup>161</sup>

Bacterial biofilms aid bacteria to evade host immune responses; they are the main source of chronic infections and can augment resistance to drug therapy.<sup>162,163</sup> Mohanty *et al.* indicated an approximately 88% decrease in biofilm formation after treatment with Ag NPs and uncovered that Ag NPs impede biofilm formation more potently compared to antimicrobial peptide LL-37.<sup>164</sup> Din *et al.* showed that the combination treatment of Ag NPs and visible blue light significantly inhibited biofilm formation by *P. aeruginosa*. *In vivo* investigations found that the number of bacteria in wounded skin dropped dramatically.<sup>160</sup>

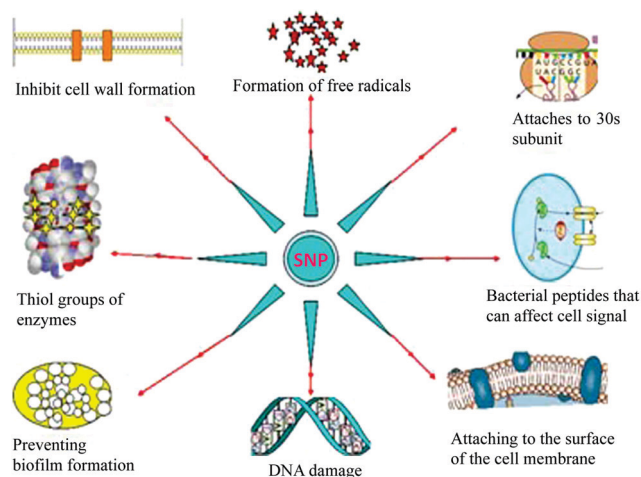


Fig. 12 Antibacterial mechanism of silver nanoparticles.<sup>147</sup>



Gurunathan *et al.* reported that Ag NPs inhibited the activity of biofilms of all the tested bacterial strains and the concentrations of Ag NPs were slightly lower than those that affected cell viability.<sup>165</sup>

In recent years, bimetallic nanoparticles (NPs), in an alloy or core-shell NP formulation, have attracted attention as a novel class of nanomaterials. It was further reported that the addition of other noble metals to silver nanoparticles is known to alter the silver dissolution behavior and reduce their overall toxicity towards eukaryotes.<sup>166</sup> Of these, noble bimetallic NPs containing gold and silver have been of immense interest. Holden *et al.* synthesized biocompatible Au/Ag alloy bimetallic nanoparticles by an alternative “green” approach and indicated that a majority of the bacterial membranes were completely disrupted by the Au/Ag alloy, causing the intracellular material to flow out.<sup>167</sup> Ding *et al.* found that Au/Ag NPs showed strong antibacterial activity (MIC as low as 7.5 pM) and negligible toxicity to human dermal fibroblasts. Moreover, Au/Ag NPs effectively removed 85% of the notorious bacterial biofilm within 4 min under NIR irradiation.<sup>168</sup> Banerjee *et al.* realized that Au/Ag core-shell NPs showed antibacterial activity against both Gram negative and Gram positive bacteria at a low concentration of silver present in the shell. TEM and flow cytometric studies indicated that the core-shell NPs attached to the bacterial surface and caused irreparable membrane damage, leading to cell death. They concluded that the enhanced antibacterial activity of Au/Ag core-shell NPs as compared to Ag NPs of similar sizes could be due to the more active silver atoms in the shell surrounding the gold core due to the high surface free energy of the surface Ag atoms owing to the shell thinness in the bimetallic NP structure.<sup>169</sup>

Another strategy for the development of novel antimicrobials is to combine the stability and pleiotropic effects of inorganic compounds with the specificity and efficiency of organic compounds. Dos Santos *et al.* added Au/Ag alloy NPs to antibiotics; a strong enhancement of the antimicrobial effect of the antibiotic was clearly observed and the dose of antibiotic necessary was considerably decreased. The observed effect was more pronounced than the sum of the individual effects of the nanoparticles and antibiotic, indicating a possible synergistic effect of the metal ions and the antibiotics possibly *via* targeting of different cell structures and physiological pathways.<sup>170</sup> Yallappa *et al.* observed that the antimicrobial activity was increased 1–2 times for ampicillin and kanamycin in the presence of Au and Ag NPs against both Gram positive and Gram negative bacteria, whereas for Au–Ag alloy NPs, the antimicrobial activity was significantly increased 3–4 times. It is clearly indicated that Au–Ag alloy NPs linked with antibiotics were more potent than Au and Ag NP linked antibiotics against all test strains.<sup>171</sup> In addition, Wang *et al.* designed and prepared a novel antibacterial nanomaterial, referred to as Au–Ag alloy NP modified SiNWAs (SN-Au/Ag). The results showed that SN-Au/Ag could kill bacteria with high efficiency in a few minutes under sunlight through synergism between photothermal and photocatalytic effects. The combination of heat and reactive oxygen species (ROS) caused bacterial death by destroying cell membranes and leaking cytoplasmic contents (Fig. 13).<sup>172</sup>

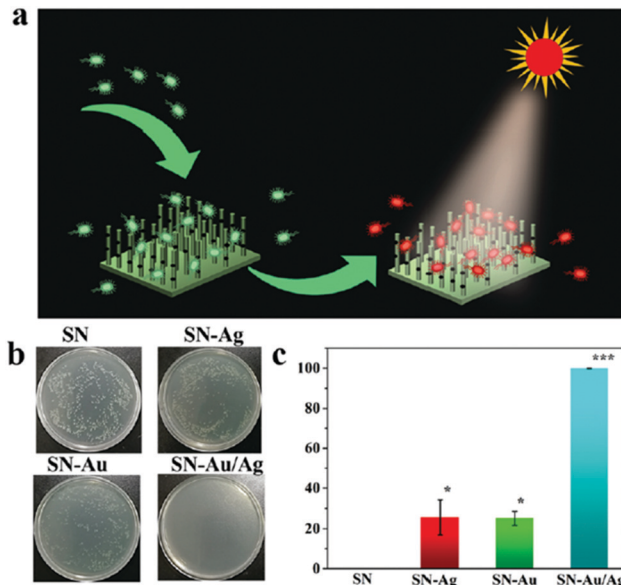


Fig. 13 Antibacterial effect of SN-Au/Ag exposed to sunlight for a short time. (a) Schematic of the method. (b) Colony formation (agar plate) by light-treated *E. coli* on different nanomaterials. (c) Bacterial killing efficiency of SN, SN-Ag, SN-Au and SN-Au/Ag after 10 min exposure to sunlight.<sup>172</sup>

## 5. Conclusions and future perspectives

The physical and chemical properties of metal nanomaterials can have a great influence on their antimicrobial activity, including the size, shape and composition of their structures.<sup>173</sup> Recent studies have found that when the size of gold nanoparticles is reduced to 2 nm, gold nanoparticles begin to catalyze the production of ROS, thus showing certain antibacterial ability.<sup>143,174</sup> Zheng *et al.* synthesized gold nanoparticles with sizes of 2 nm and 6 nm, and found that only gold nanoparticles with sizes of 2 nm could catalyze the generation of ROS and achieve an antibacterial effect.<sup>143</sup> Wang's group also found that smaller gold nanoclusters had better antibacterial properties than larger gold nanoparticles.<sup>145</sup> A size-dependent interaction between the silver nanoparticles and the bacteria was also observed. Agnihotri *et al.* noted that the smallest silver nanoparticles showed the highest antimicrobial efficiency as well as the fastest bacterial killing behavior.<sup>175</sup> In addition to the size effect, ligands may also significantly affect the antibacterial properties of nanomaterials. Zheng *et al.* reported that among four gold nanoclusters synthesized with different ligands, only AuDAMP showed strong antibacterial activity against ESKAPE.<sup>145</sup> Rotello's team found that gold nanoparticles with strong antibacterial activity and harmless to animal cells could be obtained by adjusting the structure of amphoteric ion ligands on the surface.<sup>176</sup> Concerning the shape effect on the antimicrobial activity, it is reported that the antibacterial activity of silver nanospheres was better than that of triangular nanoplates.<sup>177</sup> It suggests that the shape effect on the antibacterial activity of silver nanoparticles is attributed to the specific surface areas and facet reactivity.<sup>178</sup> Silver nanoparticles with larger effective contact areas and more reactive

facets had enhanced affinity with the cell membranes and an increased dissolution rate of silver ions, which resulted in enhanced antimicrobial activity.<sup>179,180</sup> Several reports demonstrated that Ag NPs with exposed {100} facets showed greater reactivity than ones with exposed {111} facets.<sup>178,181,182</sup>

With the application of metal nanomaterials in various fields, problems such as biosafety have gradually become a hot spot of concern. Kim *et al.* showed that with the increase of Ag NPs, cholesterol and alkaline phosphatase in SD mice increased significantly, and a high concentration of Ag NPs may cause liver damage.<sup>183</sup> In addition, studies have found that different nanoparticles have concentration-dependent toxicity to male mouse spermatogonial stem cells, and Ag NPs are the most toxic of these nanoparticles.<sup>184</sup> Some researchers also observed the effects of silver nanoparticles on lung function in SD rats, and the results showed that after treatment with Ag NPs for 90 days, the rats developed an inflammatory response that further induced changes in lung function.<sup>185</sup>

In addition to cytotoxicity, a few recent studies have provided tentative evidence of bacterial resistance or reduced susceptibility to Ag NPs.<sup>186,187</sup> Gunawan *et al.* described bacterial behavior in response to repeated long-term exposure to Ag NPs and reported that *Bacillus subtilis* had the ability to adapt to cellular oxidative stress produced by Ag<sup>+</sup>.<sup>188</sup> Panáček *et al.* also indicated that bacteria could develop resistance to silver nanoparticles after repeated exposure, and pointed out that the resistance evolves without any genetic changes; only phenotypic change is needed to reduce the nanoparticles' stability and thus eliminate the antibacterial activity of Ag NPs.<sup>189</sup> Owing to these shortcomings, the application of metal nanoparticles in clinical practice is limited. Since the invention of penicillin in 1929,<sup>190</sup> antibiotics have made tremendous contributions to the fight against various pathogens. The combination of nanomaterials and antibiotics can reduce the dosage of both, thus reducing the cytotoxicity and exerting an excellent synergistic antibacterial effect. Silver nanoparticles have been reported to significantly improve antibacterial properties when combined with antibiotics such as gentamicin. *In vivo* animal experiments further confirmed the effectiveness of the synergistic antibacterial effect.<sup>191</sup> Zheng *et al.* designed a helpful antimicrobial hybrid synthesized by conjugating Ag NPs with daptomycin, and it exhibited improved antibacterial capacity over the physically mixed Ag NPs and daptomycin.<sup>192</sup>

Au NPs have excellent antibacterial effects and diverse antibacterial mechanisms. A study also found that after bacteria were treated with Au NPs at a concentration of 33% MIC, after continuous treatment for 30 days, the bacteria remained sensitive to Au NPs under MIC treatment, suggesting that Au NPs are not susceptible to bacterial resistance.<sup>145</sup> Nevertheless, the possibility of Au NP resistance caused by repeated and long-term low concentration treatment cannot be ruled out. It has been observed that repeated treatment of bacteria with copper ions causes an increase in the expression of the bacterial copper ion efflux pump, thereby exhibiting a tendency of copper ion tolerance. Moreover, clinical application is still lacking, which requires more information on the long-term toxicity of Au NPs *in vivo*.<sup>193</sup> Au has relatively low activity and little oxidation occurs,

which means fewer free ions and ROS are produced. In order to produce excessive ROS and achieve an antibacterial effect, Au NPs of higher concentration may be required, which may reduce their biocompatibility.<sup>194,195</sup>

Determining whether nanoparticles can be modified and affected by the *in vivo* and intracellular environment is a problem that needs to be further explored and solved in future research. It is generally believed that when nanoparticles enter the human body, they will absorb negative proteins in the body, which will easily lead to aggregation and change the properties of the nanoparticles. The size, surface charge, dispersant and environment of nanoparticles not only affect their antibacterial properties, but also change the safety of metal nanoparticles. Metal NPs such as Au NPs and Ag NPs have made significant achievements in many areas; whether they can be completely safe in clinical application remains to be further proved. In the process of clinical transformation, the distribution and transportation of metal NPs and the interaction between metal NPs and biological systems need to be further understood. The size, composition, shape and aggregation rate of relevant NPs also need to be considered from organs to cells, organelles and even biological macromolecules.<sup>196</sup>

## Conflicts of interest

There are no conflicts of interests to declare.

## Acknowledgements

This work was supported by the National Natural Science Foundation of China (91753106), the Primary Research & Development Plan of Jiangsu Province (BE2019716) and the National Key Research and Development Program of China (2017YFA0205300).

## References

- 1 A. J. Huh and Y. J. Kwon, *J. Controlled Release*, 2011, **156**, 128–145.
- 2 R. Y. Pelgrift and A. J. Friedman, *Adv. Drug Delivery Rev.*, 2013, **65**, 1803–1815.
- 3 M. S. Ahmed, T. Annamalai, X. Li, A. Seddek, P. Teng, Y. C. Tse-Dinh and H. Moon, *Bioconjugate Chem.*, 2018, **29**, 1006–1009.
- 4 K. P. Miller, L. Wang, B. C. Benicewicz and A. W. Decho, *Chem. Soc. Rev.*, 2015, **44**, 7787–7807.
- 5 W. Zhang, J. Song, R. Liang, X. Zheng, J. Chen, G. Li, B. Zhang, X. Yan and R. Wang, *Bioconjugate Chem.*, 2013, **24**, 1805–1812.
- 6 J. Li, J. J. Zhu and K. Xu, *Trends Anal. Chem.*, 2014, **58**, 90–98.
- 7 L. B. Zhang and E. K. Wang, *Nano Today*, 2014, **9**, 132–157.
- 8 Y. Zhao, Y. Tian, Y. Cui, W. Liu, W. Ma and X. Jiang, *J. Am. Chem. Soc.*, 2010, **132**, 12349–12356.

- 9 G. Fang, W. Li, X. Shen, J. M. Perez-Aguilar, Y. Chong, X. Gao, Z. Chai, C. Chen, C. Ge and R. Zhou, *Nat. Commun.*, 2018, **9**, 1–9.
- 10 A. Sangsuwan, H. Kawasaki, Y. Matsumura and Y. Iwasaki, *Bioconjugate Chem.*, 2016, **27**, 2527–2533.
- 11 A. P. Richter, J. S. Brown, B. Bharti, A. Wang, S. Gangwal, K. Houck, E. A. Cohen Hubal, V. N. Paunov, S. D. Stoyanov and O. D. Velev, *Nat. Nanotechnol.*, 2015, **10**, 817–823.
- 12 Y. H. Kim, D. K. Lee, H. G. Cha, C. W. Kim, Y. H. Kang and Y. S. Kang, *J. Phys. Chem. B*, 2006, **110**, 24923–24928.
- 13 C. J. Huang, Y. S. Chen and Y. Chang, *ACS Appl. Mater. Interfaces*, 2015, **7**, 2415–2423.
- 14 J. L. Liu, L. L. Lu, S. Y. Xu and L. Y. Wang, *Talanta*, 2015, **134**, 54–59.
- 15 X. Zhang, Y. Jiang, C. Huang, J. Shen, X. Dong, G. Chen and W. Zhang, *Biosens. Bioelectron.*, 2017, **89**, 913–918.
- 16 Y. Zheng, X. Wang and H. Jiang, *Sens. Actuators, B*, 2018, **277**, 388–393.
- 17 K. K. Haldar, S. Kundu and A. Patra, *ACS Appl. Mater. Interfaces*, 2014, **6**, 21946–21953.
- 18 S. Kundu, *Phys. Chem. Chem. Phys.*, 2013, **15**, 14107–14119.
- 19 G. Chen, Q. Xu, Y. Yang, C. Li, T. Huang, G. Sun, S. Zhang, D. Ma and X. Li, *ACS Appl. Mater. Interfaces*, 2015, **7**, 23538–23544.
- 20 A. G. M. da Silva, T. S. Rodrigues, J. Wang, L. K. Yamada, T. V. Alves, F. R. Ornellas, R. A. Ando and P. H. C. Camargo, *Langmuir*, 2015, **31**, 10272–10278.
- 21 X. Xiao, H. Zhong, C. Zheng, M. Lu, X. Zuo and J. Nan, *Chem. Eng. J.*, 2016, **304**, 908–916.
- 22 R. Cai, D. Yang, K. T. Lin, T. S. Cao, Y. Lyv, K. Chen, Y. Yang, J. Ge, L. Xia, G. Christou, Y. Zhao, Z. Chen and W. Tan, *Nanoscale*, 2019, **11**, 20968–20976.
- 23 J. Ge, R. Cai, L. Yang, L. Zhang, Y. Jiang, Y. Yang, C. Cui, S. Wan, X. Chu and W. Tan, *ACS Sustainable Chem. Eng.*, 2018, **6**, 16555–16562.
- 24 J. B. Jackson and N. J. Halas, *J. Phys. Chem. B*, 2001, **105**, 2743–2746.
- 25 Y. Xia and N. J. Halas, *MRS Bull.*, 2004, **30**, 338–348.
- 26 M. Faraday, *Philos. Trans.*, 1857, **147**, 145–181.
- 27 J. Turkevich, P. C. Stevenson and J. Hillier, *Discuss. Faraday Soc.*, 1951, **11**, 55–75.
- 28 X. Ji, X. Song, J. Li, Y. Bai, W. Yang and X. Peng, *J. Am. Chem. Soc.*, 2007, **129**, 13939–13948.
- 29 H. Xia, S. Bai, J. Hartmann and D. Wang, *Langmuir*, 2010, **26**, 3585–3589.
- 30 V. K. Lamer and R. H. Dinegar, *J. Am. Chem. Soc.*, 1950, **72**, 4847–4854.
- 31 C. Ziegler and A. Eychmüller, *J. Phys. Chem. C*, 2011, **115**, 4502–4506.
- 32 D. Rioux and M. Meunier, *J. Phys. Chem. C*, 2015, **119**, 13160–13168.
- 33 J. Rodríguez-Fernández, J. Pérez-Juste, F. J. García de Abajo and L. M. Liz-Marzán, *Langmuir*, 2006, **22**, 7007–7010.
- 34 N. G. Bastús, J. Comenge and V. Puntes, *Langmuir*, 2011, **27**, 11098–11105.
- 35 X. Liu, H. Xu, H. Xia and D. Wang, *Langmuir*, 2012, **28**, 13720–13726.
- 36 N. R. Jana, L. Gearheart and C. J. Murphy, *J. Phys. Chem. B*, 2001, **105**, 4065–4067.
- 37 B. D. Busbee, S. O. Obare and C. J. Murphy, *Adv. Mater.*, 2003, **15**, 414–416.
- 38 H. Y. Wu, W. L. Huang and M. H. Huang, *Cryst. Growth Des.*, 2007, **7**, 831–835.
- 39 H. Y. Wu, H. C. Chu, T. J. Kuo, C. L. Kuo and M. H. Huang, *Chem. Mater.*, 2005, **17**, 6447–6451.
- 40 B. Nikoobakht and M. A. El-sayed, *Chem. Mater.*, 2003, **15**, 1957–1962.
- 41 N. R. Jana, *Small*, 2005, **1**, 875–882.
- 42 K. Park, L. F. Drummy, R. C. Wadams, H. Koerner, D. Nepal, L. Fabris and R. A. Vaia, *Chem. Mater.*, 2013, **25**, 555–563.
- 43 T. Wen, Z. Hu, W. Liu, H. Zhang, S. Hou, X. Hu and X. Wu, *Langmuir*, 2012, **28**, 17517–17523.
- 44 X. Ye, L. Jin, H. Caglayan, J. Chen, G. Xing, C. Zheng, V. Doan-Nguyen, Y. Kang, N. Engheta, C. R. Kagan and C. B. Murray, *ACS Nano*, 2012, **6**, 2804–2817.
- 45 X. Ye, C. Zheng, J. Chen, Y. Gao and C. B. Murray, *Nano Lett.*, 2013, **13**, 765–771.
- 46 X. C. Jiang, A. Brioude and M. P. Pileni, *Colloids Surf.*, 2006, **277**, 201–206.
- 47 J. Zheng, C. Zhou, M. Yu and J. Liu, *Nanoscale*, 2012, **4**, 4073–4083.
- 48 X. Jiang, B. Du, Y. Huang and J. Zheng, *Nano Today*, 2018, **21**, 106–125.
- 49 Y. Negishi, N. K. Chaki, Y. Shichibu, R. L. Whetten and T. Tsukuda, *J. Am. Chem. Soc.*, 2007, **129**, 11322–11323.
- 50 Y. Shichibu, Y. Negishi, H. Tsunoyama, M. Kanehara, T. Teranishi and T. Tsukuda, *Small*, 2007, **3**, 835–839.
- 51 J. Zheng, C. W. Zhang and R. M. Dickson, *Phys. Rev. Lett.*, 2004, **93**, 7–13.
- 52 G. B. Santiago, M. J. Rodríguez, C. Blanco, J. Rivas, M. A. López-Quintela and J. M. Martinho, *Nano Lett.*, 2010, **10**, 4217–4221.
- 53 J. Xie, Y. Zheng and J. Y. Ying, *J. Am. Chem. Soc.*, 2009, **131**, 888–889.
- 54 H. Wei, Z. Wang, L. Yang, S. Tian, C. Hou and Y. Lu, *Analyst*, 2010, **135**, 1406–1410.
- 55 G. Liu, Y. Shao, K. Ma, Q. Cui, F. Wu and S. Xu, *Gold Bull.*, 2012, **45**, 69–74.
- 56 T. Qing, X. He, D. He, Z. Qing, K. Wang, Y. Lei, T. Liu, P. Tang and Y. Li, *Talanta*, 2016, **161**, 170–176.
- 57 H. Kawasaki, K. Hamaguchi, I. Osaka and R. Arakawa, *Adv. Funct. Mater.*, 2011, **21**, 3508–3515.
- 58 K. Chaudhari, P. L. Xavier and T. Pradeep, *ACS Nano*, 2011, **5**, 8816–8827.
- 59 J. Liu, J. Chen and X. Yan, *Anal. Chem.*, 2013, **85**, 3238–3245.
- 60 L. Wang, G. Chen, G. Zeng, J. Liang, H. Dong, M. Yan, Z. Li, Z. Guo, W. Tao and L. Peng, *New J. Chem.*, 2015, **39**, 9306–9312.
- 61 J. Wang, G. Zhang, Q. Li, H. Jiang, C. Liu, C. Amatore and X. Wang, *Sci. Rep.*, 2013, **3**, 1157.
- 62 M. Wang, Y. Chen, W. Cai, H. Feng, T. Du, W. Liu, H. Jiang, A. Pasquarelli, Y. Weizmann and X. Wan, *Proc. Natl. Acad. Sci. U. S. A.*, 2020, **117**, 308–316.



- 63 M. Wang, Z. Yu, H. Feng, J. Wang, L. Wang, Y. Zhang, L. Yin, Y. Du, H. Jiang, X. Wang and J. Zhou, *J. Mater. Chem. B*, 2019, **7**, 5336–5344.
- 64 U. Goswami, A. K. Sahoo, A. Chattopadhyay and S. S. Ghosh, *ACS Omega*, 2018, **3**, 6113–6119.
- 65 H. M. Chen, R. S. Liu and D. P. Tsai, *Cryst. Growth Des.*, 2009, **9**, 2079–2087.
- 66 Y. Shao, Y. Jin and S. Dong, *Chem. Commun.*, 2004, 1104–1105.
- 67 Y. Sun and Y. Xia, *Science*, 2003, **34**, 2176–2179.
- 68 S. Chen, L. W. Zhong, J. Ballato, S. H. Foulger and D. L. Carroll, *J. Am. Chem. Soc.*, 2003, **125**, 16186–16187.
- 69 C. Zhu, G. Meng, Q. Huang, Z. Huang and Z. Chu, *Cryst. Growth Des.*, 2011, **11**, 748–752.
- 70 S. T. Selvan, *Chem. Commun.*, 1998, 351–352.
- 71 J. P. Xiao, Y. Xie, R. Tang, M. Chen and X. B. Tian, *Adv. Mater.*, 2001, **13**, 1887–1891.
- 72 Z. An, J. Zhang and S. Pan, *CrystEngComm*, 2010, **12**, 500–506.
- 73 M. Yamamoto, Y. Kashiwagi, T. Sakata, H. Mori and M. Nakamoto, *Chem. Mater.*, 2005, **17**, 5391–5393.
- 74 B. Wiley, Y. Sun, B. Mayers and Y. Xia, *Chem. – Eur. J.*, 2005, **11**, 454–463.
- 75 X. Z. Lin, X. W. Teng and H. Yang, *Langmuir*, 2003, **19**, 10081–10085.
- 76 N. R. Jana, L. Gearheart and C. J. Murphy, *Chem. Commun.*, 2001, 617–618.
- 77 R. C. Jin, Y. W. Cao and C. A. Mirkin, *Science*, 2001, **294**, 1901–1903.
- 78 B. J. Wiley, Y. J. Xiong and Z. Y. Li, *Nano Lett.*, 2006, **6**, 765–768.
- 79 Y. J. Chao, Y. P. Lyu, Z. W. Wu and C. L. Lee, *Energy*, 2016, **41**, 3896–3903.
- 80 Y. M. Chang, I. T. Lu, C. Y. Chen, Y. C. Hsieh and P. W. Wu, *J. Alloys Compd.*, 2014, **586**, 507–511.
- 81 S. H. Im, Y. T. Lee, B. Wiley and Y. Xia, *Angew. Chem., Int. Ed.*, 2005, **44**, 2154–2157.
- 82 S. E. Skrabalak, L. Au, X. Li and Y. Xia, *Nat. Protoc.*, 2007, **2**, 2182–2190.
- 83 Y. Wang, Y. Zheng, C. Huang and Y. Xia, *J. Am. Chem. Soc.*, 2013, **135**, 1941–1951.
- 84 S. J. Jeon, J. H. Lee and E. L. Thomas, *J. Colloid Interface Sci.*, 2014, **435**, 105–111.
- 85 E. Braun, Y. Eichen, U. Sivan and G. Ben-Yoseph, *Nature*, 1998, **391**, 775–778.
- 86 S. H. Park, R. Barish, H. Li, J. H. Reif, G. Finkelstein, H. Yan and T. H. LaBean, *Nano Lett.*, 2005, **5**, 693–696.
- 87 R. Yang, C. Sui, J. Gong and L. Qu, *Mater. Lett.*, 2007, **61**, 900–903.
- 88 B. H. Hong, S. C. Bae, C. W. Lee, S. Jeong and K. S. Kim, *Science*, 2001, **294**, 348–351.
- 89 K. S. Kim, *Curr. Appl. Phys.*, 2002, **2**, 65–69.
- 90 D. Zhang, L. Qi, J. Yang, J. Ma, H. Cheng and H. Lan, *Chem. Mater.*, 2004, **16**, 872–876.
- 91 D. Zhang, L. Qi, J. Ma and H. Cheng, *Chem. Mater.*, 2001, **13**, 2753–2755.
- 92 Z. Wang, J. Liu, X. Chen, J. Wang and Y. Qian, *Chem. – Eur. J.*, 2010, **11**, 160–163.
- 93 K. K. Caswell, C. M. Bender and C. J. Murphy, *Nano Lett.*, 2003, **3**, 667–669.
- 94 Y. Sun, Y. Yin, B. T. Mayers, T. Herricks and Y. Xia, *Chem. Mater.*, 2002, **14**, 4736–4745.
- 95 B. Wiley, T. Herricks, Y. Sun and Y. Xia, *Nano Lett.*, 2004, **4**, 1733–1739.
- 96 K. E. Korte, S. E. Skrabalak and Y. Xia, *J. Mater. Chem.*, 2008, **18**, 437–441.
- 97 J. Ma and M. Zhan, *RSC Adv.*, 2014, **4**, 21060–21071.
- 98 J. H. Lee, P. Lee, D. Lee, S. S. Lee and S. H. Ko, *Cryst. Growth Des.*, 2012, **12**, 5598–5605.
- 99 Y. Ran, W. He, K. Wang, S. Ji and C. Ye, *Chem. Commun.*, 2014, **50**, 14877–14880.
- 100 G. A. Ozin, R. Hugues, S. M. Mattar and D. F. Mcintosh, *J. Phys. Chem.*, 1983, **87**, 3445–3450.
- 101 M. D. Baker, G. A. Ozin and J. Godber, *J. Phys. Chem.*, 1985, **89**, 305–311.
- 102 T. Sun and K. Seff, *Chem. Rev.*, 1994, **94**, 857–870.
- 103 L. Konig, I. Rabin, W. Schulze and G. Ertl, *Science*, 1996, **274**, 1353–1355.
- 104 I. Rabin, W. Schulze and G. Ertl, *J. Chem. Phys.*, 1998, **108**, 5137–5142.
- 105 I. Rabin, W. Schulze and G. Ertl, *Chem. Phys. Lett.*, 1999, **312**, 394–398.
- 106 O. N. Bilan, V. A. Tyurnin, N. G. Cherenda, A. V. Shendrik and D. M. Yudin, *J. Appl. Spectrosc.*, 1980, **33**, 717–720.
- 107 E. Borsella, E. Cattaruzza, G. D. Marchi, R. Gonella, G. Mattei, P. Mazzoldi, A. Quaranta, G. Battaglin and R. Polloni, *J. Non-Cryst. Solids*, 1999, **245**, 122–128.
- 108 T. Linnert, P. Mulvaney, A. Henglein and H. Weller, *J. Am. Chem. Soc.*, 1990, **112**, 4657–4664.
- 109 A. Henglein, P. Mulvaney and T. Linnert, *Faraday Discuss.*, 1991, **92**, 31–44.
- 110 P. Mulvaney, T. Linnert and A. Henglein, *J. Phys. Chem.*, 1991, **95**, 7843–7846.
- 111 B. G. Ershov, E. Janata and A. Henglein, *J. Phys. Chem.*, 1993, **97**, 339–343.
- 112 B. G. Ershov, E. Janata, A. Henglein and A. Fojtik, *J. Phys. Chem.*, 1993, **97**, 4589–4594.
- 113 A. Henglein, *J. Phys. Chem.*, 1993, **97**, 5457–5471.
- 114 B. G. Ershov and A. Henglein, *J. Phys. Chem. B*, 1998, **102**, 10663–10666.
- 115 J. Zheng and R. M. Dickson, *J. Am. Chem. Soc.*, 2002, **124**, 13982–13983.
- 116 W. Lesniak, A. U. Bielinska, K. Sun, K. W. Janczak, X. Shi, J. R. Baker and L. P. Balogh, *Nano Lett.*, 2005, **5**, 2123–2130.
- 117 L. Shang and S. J. Dong, *Chem. Commun.*, 2008, 1088–1090.
- 118 L. Shang and S. J. Dong, *J. Mater. Chem.*, 2008, **18**, 4636–4640.
- 119 S. Liu, F. Lu and J. Zhu, *Chem. Commun.*, 2011, **47**, 2661–2663.
- 120 Z. Yuan, N. Cai, Y. Du, Y. He and E. S. Yeung, *Anal. Chem.*, 2014, **86**, 419–426.
- 121 Z. Wu, E. Lanni, W. Chen, M. E. Bier, D. Ly and R. Jin, *J. Am. Chem. Soc.*, 2009, **131**, 16672–16674.
- 122 B. Adhikari and A. Baneqee, *Chem. Mater.*, 2010, **22**, 4364–4371.

- 123 T. Udaya Bhaskara Rao and T. Pradeep, *Angew. Chem., Int. Ed.*, 2010, **49**, 3925–3929.
- 124 T. U. B. Rao, B. Nataraju and T. Pradeep, *J. Am. Chem. Soc.*, 2010, **132**, 16304–16307.
- 125 X. Yuan, Z. Luo, Q. Zhang, X. Zhang, Y. Zheng, J. Y. Lee and J. Xie, *ACS Nano*, 2011, **5**, 8800–8808.
- 126 J. Zhu, X. Song, L. Gao, Z. Li, Z. Liu, S. Ding, S. Zou and Y. He, *Biosens. Bioelectron.*, 2014, **53**, 71–75.
- 127 R. M. Izatt, J. J. Christensen and J. H. Rytting, *Chem. Rev.*, 1971, **71**, 439–481.
- 128 J. T. Petty, J. Zheng, N. V. Hud and R. M. Dickson, *J. Am. Chem. Soc.*, 2004, **126**, 5207–5212.
- 129 C. I. Richards, S. Choi, J. C. Hsiang, Y. Antoku, T. Vosch, A. Bongiorno, Y. L. Tzeng and R. M. Dickson, *J. Am. Chem. Soc.*, 2008, **130**, 5038–5039.
- 130 H. Eun, W. Y. Kwon, K. Kalimuthu, Y. Kim, M. Lee, J. O. Ahn, H. Lee, S. H. Lee, H. J. Kim, H. G. Park and K. S. Park, *J. Mater. Chem. B*, 2019, **7**, 2512–2517.
- 131 W. Guo, J. Yuan, Q. Dong and E. Wang, *J. Am. Chem. Soc.*, 2010, **132**, 932–934.
- 132 K. Ma, Q. Cui, G. Liu, F. Wu, S. Xu and Y. Shao, *Nanotechnology*, 2011, **22**, 305502.
- 133 E. G. Gwinn, P. O'Neill, A. J. Guerrero, D. Bouwmeester and D. K. Fygenson, *Adv. Mater.*, 2008, **20**, 279–283.
- 134 Y. Cui, Y. Zhao, Y. Tian, W. Zhang, X. Lu and X. Jiang, *Biomaterials*, 2012, **33**, 2327–2333.
- 135 S. C. Hayden, G. Zhao, K. Saha, R. L. Phillips, X. Li, O. R. Miranda, V. M. Rotello, M. A. El-Sayed, I. Schmidt-Krey and U. H. F. Bunz, *J. Am. Chem. Soc.*, 2012, **134**, 6920–6923.
- 136 X. Li, S. M. Robinson, A. Gupta, K. Saha, Z. Jiang, D. F. Moyano, A. Sahar, M. A. Riley and V. M. Rotello, *ACS Nano*, 2014, **8**, 10682–10691.
- 137 W. Y. Chen, H. Y. Chang, J. K. Lu, Y. C. Huang, S. G. Harroun, Y. T. Tseng, Y. J. Li, C. C. Huang and H. T. Chang, *Adv. Funct. Mater.*, 2015, **25**, 7189–7199.
- 138 A. Rai, A. Prabhune and C. C. Perry, *J. Mater. Chem.*, 2010, **20**, 6789–6798.
- 139 G. Mendoza, A. Regiel-Futyra, V. Andreu, V. Sebastian, A. Kyziol, G. Stochel and M. Arruebo, *ACS Appl. Mater. Interfaces*, 2017, **9**, 17693–17701.
- 140 X. Yang, J. Yang, L. Wang, B. Ran, Y. Jia, L. Zhang, G. Yang, H. Shao and X. Jiang, *ACS Nano*, 2017, **11**, 5737–5745.
- 141 G. L. Burygin, B. N. Khlebtsov, A. N. Shantrokha, L. A. Dykman, V. A. Bogatyrev and N. G. Khlebtsov, *Nanoscale Res. Lett.*, 2009, **4**, 794–801.
- 142 Y. Zheng, W. Liu, Y. Chen, C. Li, H. Jiang and X. Wang, *J. Colloid Interface Sci.*, 2019, **546**, 1–10.
- 143 K. Zheng, M. I. Setyawati, D. T. Leong and J. Xie, *ACS Nano*, 2017, **11**, 6904–6910.
- 144 W. Bing, H. Sun, F. Wang, Y. Song and J. Ren, *J. Mater. Chem. B*, 2018, **6**, 4602–4609.
- 145 Y. Zheng, W. Liu, Z. Qin, Y. Chen, H. Jiang and X. Wang, *Bioconjugate Chem.*, 2018, **29**, 3094–3103.
- 146 Y. Xie, Y. Liu, J. Yang, Y. Liu, F. Hu, K. Zhu and X. Jiang, *Angew. Chem., Int. Ed.*, 2018, **57**, 3958–3962.
- 147 M. K. Rai, S. D. Deshmukh, A. P. Ingle and A. K. Gade, *J. Appl. Microbiol.*, 2012, **11**, 841–852.
- 148 K. Kawata, M. Osawa and S. Okabe, *Environ. Sci. Technol.*, 2009, **43**, 6046–6051.
- 149 E. Navarro, F. Piccapietra, B. Wagner, F. Marconi, R. Kaegi, N. Odzak, L. Sigg and R. Behra, *Environ. Sci. Technol.*, 2008, **42**, 8959–8964.
- 150 H. T. Ratte, *Environ. Toxicol. Chem.*, 1999, **18**, 89–108.
- 151 J. Y. Bottero, M. Auffan, J. Rose, C. Mouneyrac, C. Botta, J. Labille, A. Masion, A. Thill and C. Chaneac, *C. R. Geosci.*, 2011, **343**, 168–176.
- 152 R. Kumar and H. Munstedt, *Biomaterials*, 2005, **26**, 2081–2088.
- 153 S. Kim and D. Y. Ryu, *J. Appl. Toxicol.*, 2013, **33**, 78–89.
- 154 M. Danilczuk, A. Lund, J. Sadlo, H. Yamada and J. Michalik, *Spectrochim. Acta, Part A*, 2006, **63**, 189–191.
- 155 J. S. Kim, E. Kuk, K. N. Yu, J. H. Kim, S. J. Park, H. J. Lee, S. H. Kim, Y. K. Park, Y. H. Park, C. Y. Hwang, Y. K. Kim, Y. S. Lee, D. H. Jeong and M. H. Cho, *Nanomedicine*, 2007, **3**, 95–101.
- 156 C. E. Escárcega-Gonzál, J. A. Garza-Cervantes, A. Vázquez-Rodríguez, L. Z. Montelongo-Peralta, M. T. Treviño-González, E. D. B. Castro, E. M. Saucedo-Salazar, R. M. Chávez Morales, D. I. R. Soto, F. M. T. González, J. L. C. Rosales, R. V. Cruz and J. R. Morones-Ramírez, *Int. J. Nanomed.*, 2018, **13**, 2349–2363.
- 157 M. Raffi, F. Hussain, T. Bhatti, J. I. Akhter, A. Hameed and M. M. Hasan, *J. Mater. Sci. Technol.*, 2008, **24**, 192–196.
- 158 J. R. Morones, J. L. Elechiguerra, A. Camacho, K. Holt, J. B. Kouri, J. T. Ramirez and M. J. Yacaman, *Nanotechnology*, 2005, **16**, 2346–2353.
- 159 I. Sondi and B. Salopek-Sondi, *J. Colloid Interface Sci.*, 2004, **275**, 177–182.
- 160 S. N. E. I. Din, T. A. El-Tayeb, K. Abou-Aisha and M. El-Azizi, *Int. J. Nanomed.*, 2016, **11**, 1749–1758.
- 161 W. Li, X. Xie, Q. Shi, H.-Y. Zeng, Y. Ouyang and Y. Chen, *Appl. Microbiol. Biotechnol.*, 2010, **85**, 1115–1122.
- 162 Y. Zheng, W. Liu, Y. Chen, H. Jiang, H. Yan, I. Kosenko, L. Chekulaeva, I. Sivaev, V. Bregadze and X. Wang, *Organometallics*, 2017, **36**, 3484–3490.
- 163 N. Høiby, T. Bjarnsholt, M. Givskov, S. Molin and O. Ciofu, *Int. J. Antimicrob. Agents*, 2010, **35**, 322–332.
- 164 S. Mohanty, S. Mishra, P. Jena, B. Jacob, B. Sarkar and A. Sonawane, *Nanomedicine*, 2012, **8**, 916–924.
- 165 S. Gurunathan, J. W. Han, D.-N. Kwon and J.-H. Kim, *Nanoscale Res. Lett.*, 2014, **9**, 373.
- 166 N. Alissawi, V. Zaporojtchenko, T. Strunskus, I. Kocbas, V. S. K. Chakravadhanula, L. Kienle, D. Garbe-Schonberg and F. Faupel, *Gold Bull.*, 2013, **46**, 3–11.
- 167 M. S. Holden, J. Black, A. Lewis, M. C. Boutrín, E. Walemba, T. S. Sabir, D. S. Boskovic, A. Wilson, H. M. Fletcher and C. C. Perry, *J. Nanomater.*, 2016, **53**, 1–11.
- 168 X. Ding, P. Yuan, N. Gao, H. Z. Meng, Y. Y. Yang and Q. H. Xu, *Nanomedicine*, 2017, **13**, 297–305.
- 169 M. Banerjee, S. Sharma, A. Chattopadhyay and S. S. Ghosh, *Nanoscale*, 2011, **3**, 5120–5125.
- 170 M. M. dos Santos, M. J. Queiroz and P. V. Baptista, *J. Nanopart. Res.*, 2012, **14**, 859.

- 171 S. Yallappa, J. Manjanna and B. L. Dhananjaya, *Spectrochim. Acta, Part A*, 2015, **137**, 236–243.
- 172 Z. Wang, X. Huang, S. Jin, H. Wang, L. Yuan and J. L. Brash, *J. Mater. Chem. B*, 2019, **7**, 6202–6209.
- 173 C. Marambio-Jones and E. M. Hoek, *J. Nanopart. Res.*, 2010, **12**, 1531–1551.
- 174 K. Zheng, M. I. Setyawati, D. T. Leong and J. Xie, *Chem. Mater.*, 2018, **30**, 2800–2808.
- 175 S. Agnihotri, S. Mukherji and S. Mukherji, *RSC Adv.*, 2014, **4**, 3974–3983.
- 176 S. Huo, Y. Jiang, A. Gupta, Z. Jiang, R. F. Landis, S. Hou, X. Liang and V. M. Rotello, *ACS Nano*, 2016, **10**, 8732–8737.
- 177 M. J. Gao, L. Sun, Z. Q. Wang and Y. B. Zhao, *Mater. Sci. Eng., C*, 2013, **33**, 397–404.
- 178 X. Hong, J. Wen, X. Xiong and Y. Hu, *Environ. Sci. Pollut. Res.*, 2016, **23**, 4489–4497.
- 179 M. Rojas-Andrade, A. T. Cho, P. G. Hu, S. J. Lee, C. P. Deming, S. W. Sweeney, C. Saltikov and S. W. Chen, *J. Mater. Sci.*, 2015, **50**, 2849–2858.
- 180 I. Vukoje, V. Lazic, V. Vodnik, M. Mitric, B. Jokic, S. P. Ahrenkiel, J. M. Nedeljkovic and M. Radetic, *J. Mater. Sci.*, 2014, **49**, 4453–4460.
- 181 S. Agarwal, L. Lefferts, B. L. Mojet, D. Ligthart, E. J. M. Hensen, D. R. G. Mitchell, W. J. Erasmus, B. G. Anderson, E. J. Olivier, J. H. Neethling and A. K. Datye, *ChemSusChem*, 2013, **6**, 1898–1906.
- 182 C. L. Lee, Y. L. Tsai, C. H. Huang and K. L. Huang, *Electrochem. Commun.*, 2013, **29**, 37–40.
- 183 Y. S. Kim, J. S. Kim, H. S. Cho, D. S. Rha, J. M. Kim, J. D. Park, B. S. Choi, R. Lim, H. K. Chang, Y. H. Chung, H. Kwon, J. Jeong, B. S. Han and J. Ye, *Inhalation Toxicol.*, 2008, **20**, 575–583.
- 184 L. Braydich-Stolle, S. Hussain, J. J. Schlager and M. C. Hofmann, *Toxicol. Sci.*, 2005, **88**, 412–419.
- 185 J. H. Sung, J. H. Ji, J. U. Yoon, D. S. Kim, M. Y. Song, J. Jeong, B. S. Han, J. H. Han, Y. H. Chung, J. Kim, T. S. Kim, H. K. Chang, E. J. Lee, J. H. Lee and J. Ye, *Inhalation Toxicol.*, 2008, **20**, 567–574.
- 186 J. L. Graves, Jr, M. Tajkarimi, Q. Cunningham, A. Campbell, H. Nonga, S. H. Harrison and J. E. Barrick, *Front. Genet.*, 2015, **6**, 42.
- 187 C. Losasso, S. Belluco, V. Cibin, P. Zavagnin, I. Mičetić, F. Gallochio, M. Zanella, L. Bregoli, G. Biancotto and A. Ricci, *Front. Microbiol.*, 2014, **5**, 227.
- 188 C. Gunawan, W. Y. Teoh, C. P. Marquis and R. Amal, *Small*, 2013, **9**, 3554–3560.
- 189 A. Panáček, L. Kvítek, M. Smékalová, R. Večeřová, M. Kolář, M. Röderová, F. Dyčka, M. Šebela, R. Prucek, O. Tomanec and R. Zbořil, *Nat. Nanotechnol.*, 2018, **13**, 65–71.
- 190 A. Fleming, *Br. J. Exp. Pathol.*, 1929, **10**, 226–236.
- 191 N. Xu, H. Cheng, J. Xu, F. Li, B. Gao, Z. Li, C. Gao, K. Huo, J. Fu and W. Xiong, *Int. J. Nanomed.*, 2017, **12**, 731–743.
- 192 K. Zheng, M. I. Setyawati, T.-P. Lim, D. T. Leong and J. Xie, *ACS Nano*, 2016, **10**, 7934–7942.
- 193 Y. Wu, M. R. K. Alia, K. Chen, N. Fang and M. A. El-Sayed, *Nano Today*, 2019, **24**, 120–140.
- 194 Y. Zhang, T. P. Shareena Dasari, H. Deng and H. Yu, *J. Environ. Sci. Health, Part C: Environ. Carcinog. Ecotoxicol. Rev.*, 2015, **33**, 286–327.
- 195 C. Zhang, Z. Hu and B. Deng, *Water Res.*, 2016, **88**, 403–427.
- 196 C. Bao, J. Conde, E. Polo, P. del Pino, M. Moros, P. V. Baptista, V. Grazu, D. Cui and J. M. de la Fuente, *Nanomedicine*, 2014, **9**, 2353–2370.